Bioorganic & Medicinal Chemistry Letters 21 (2011) 3095–3098

Contents lists available at ScienceDirect

Bioorganic & Medicinal Chemistry Letters

journal homepage: www.elsevier.com/locate/bmcl

1,5-Substituted nipecotic amides: Selective PDE8 inhibitors displaying diastereomer-dependent microsomal stability

Michael P. DeNinno [†,*], Stephen W. Wright, Michael S. Visser [‡], John B. Etienne, Dianna E. Moore, Thanh V. Olson, Benjamin N. Rocke, Melissa P. Andrews, Cynthia Zarbo, Michele L. Millham, Brian P. Boscoe, David D. Boyer, Shawn D. Doran, Karen L. Houseknecht [§]

Pfizer Global Research and Development, Eastern Point Road, Groton, CT 06340, USA

ARTICLE INFO

Article history:
Received 14 January 2011
Revised 4 March 2011
Accepted 7 March 2011
Available online 11 March 2011

Keywords:
Phosphodiesterase 8
Pancreas
Diabetes
Microsomal stability

ABSTRACT

The first highly potent and selective PDE8 inhibitors are disclosed. The initial tetrahydroisoquinoline hit was transformed into a nipecotic amide series in order to address a reactive metabolite issue. Reduction of lipophilicity to address metabolic liabilities uncovered an interesting diastereomer-dependent trend in turnover by human microsomes.

Phosphodiesterase 8B is a cAMP-specific isoform of the broader class of phosphodiesterases (PDEs).[1–3] Although mRNA for the closely related PDE8A has been found at low levels in most tissues, PDE8B is more highly expressed in the brain, thyroid, pancreas and adrenal cortex.[4,5] Expression of the enzyme in pancreatic β-cells[4] suggested that inhibition of PDE8B might have therapeutic utility in the treatment of diabetes. Such an agent could be used as a mono-therapy, or in combination with drugs which signal through cAMP such as those that act on the GLP-1 receptor.[6] Other PDE isoforms expressed in the pancreas include PDE1C, PDE3B, PDE4 and PDE10.[7] As no selective PDE8 inhibitors had been reported, a high throughput screen (HTS) was conducted with the goal of identifying selective tools for exploring the in vitro and in vivo phenotype of PDE8B inhibition.

The majority of hits from the HTS contained classical PDE pharmacophores, such as the non-selective cAMP mimic inhibitor IBMX (Fig. 1). One hit (**1**) based on a tetrahydroisoquinoline (THIQ) scaffold looked particularly attractive due to its structural novelty. It

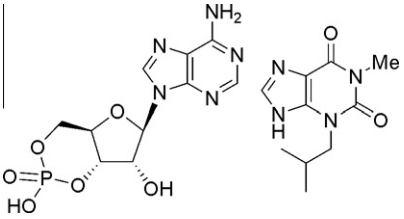

Figure 1. Structures of cAMP and IBMX.

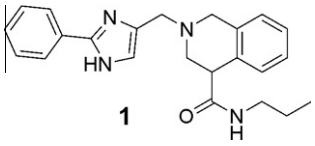

Figure 2. Structure of THIQ screening hit **1**.

was hoped that this structural novelty would result in greater specificity for derivatives of **1** against the PDE8B isozyme (Fig. 2).[8]

A standard SAR campaign around **1** gave **2** which had high potency against PDE8B (IC_{50} = 5 nM) and excellent selectivity.[9] However, it was determined that multiple analogs were positive in a glutathione adduct-based reactive metabolite assay, presumably at least partially through compound **3** which was detected as one of the major products upon microsomal incubation (Fig. 3).[10]

* Corresponding author. Tel.: +1 858 404 6664; fax: +1 858 404 6719.
E-mail address: mike_deninno@sd.vrtx.com (M.P. DeNinno).
† Present address: Vertex Pharmaceuticals Inc., 11010 Torreyana Rd., San Diego, CA 92121, USA
‡ Present address: Novartis Institutes for BioMedical Research, Inc., 250 Massachusetts Ave., Cambridge, MA 02139, USA
§ Present address: University of New England, 716 Stevens Ave., Portland, ME 04103, USA

0960-894X/$ - see front matter © 2011 Elsevier Ltd. All rights reserved.
doi:10.1016/j.bmcl.2011.03.022

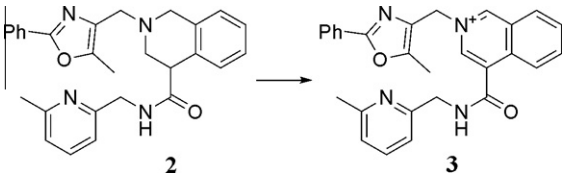

Figure 3. Structures of analog **2** and microsomal metabolite **3**.

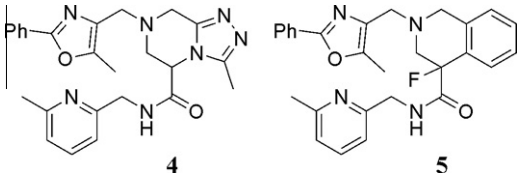

Figure 4. Structure of heterocycle **4** and fluorinated THIQ analog **5**.

We then directed our efforts upon solving the reactive metabolite problem by any of three means: (i) replacement of the fused aryl ring with more polar fused rings, (ii) blocking potential sites of metabolism on the isoquinoline, and (iii) elimination of the fused aryl ring.

The first strategy failed to afford compounds with PDE8B inhibitory activity (e.g., analog **4**). Blocking of the isoquinoline 4-position with a fluorine atom to afford **5** resulted in a 75-fold loss of potency (IC_{50} = 370 nM) without significantly improving metabolic stability (Fig. 4).

Elimination of the fused ring to reduce overall lipophilicity and reduce the driving force for metabolism to the isoquinolonium species **3**, could be accomplished with a reduction in potency. However, PDE8B inhibition potency was strongly influenced by even small structural changes (Table 1).

Substitution of the piperidine ring was explored to improve the potency of the nipecotate template **6**. These compounds were prepared as shown in Scheme 1. This route was designed to afford primarily the *cis* isomers, which preliminary modeling suggested should better mimic the THIQ template. Yields were generally good; following hydrogenation and amide bond formation, the separable *cis*/*trans* isomers were isolated in ratios of 3:1 to 10:1 depending on the substituent R^1.

We were surprised to find that the *cis* isomers were uniformly inactive (IC_{50} >2000 nM, data not shown), whereas the *trans* isomers were the active diastereomers (Table 2).[11]

Table 1
PDE8B activity of analogs lacking a fused ring

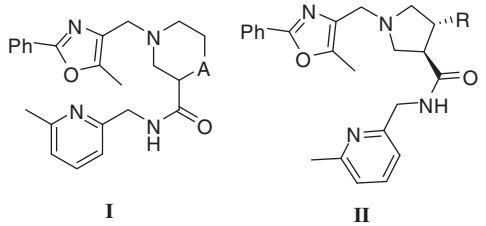

Compound	Structure	A	IC_{50} (nM)	*c* log *D*
6	**I**	CH_2	240	2.9
7	**I**	O	>10,000	2.9
8	**I**	SO_2	2400	2.1
9	**II**	H	>10,000	2.7
10	**II**	CF_3	1700	3.4

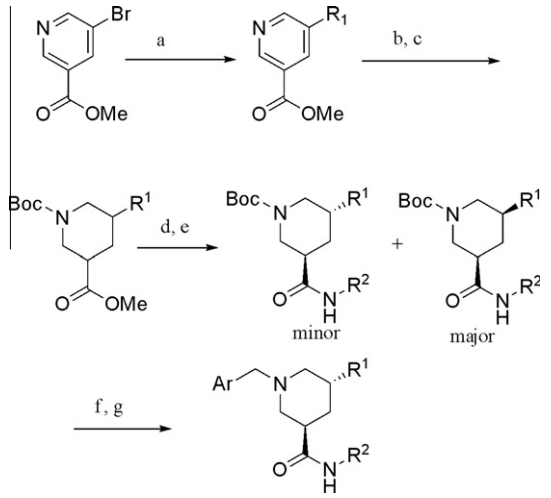

Scheme 1. Preparation of 5-substituted nipecotic amide analogs. Reagents and conditions: (a) R^1ZnX (1.5 equiv), $Pd(dppf)Cl_2$ (0.025 equiv), THF, 50 °C, 3 h; (b) H_2 (50 psi), PtO_2, H_2SO_4, EtOH, 20 °C, 24 h; (c) Boc_2O (1.5 equiv), iPr$_2$NEt (3 equiv), dioxane, 20 °C, 18 h;. (d) NaOH (2 equiv), MeOH, reflux, 18 h; (e) R^2NH_2 (1 equiv), propanephosphonic anhydride (1.2 equiv), Et_3N (3 equiv), DMF, 20 °C, 18 h; (f) HCl (5 equiv), Et_2O, MeOH, 20 °C, 2 h; (g) $ArCH_2Cl$ (1.5 equiv), iPr$_2$NEt (5 equiv), MeCN, 20 °C, 18 h.

Table 2
PDE8B activity of *trans*-5-substituted nipecotate analogs

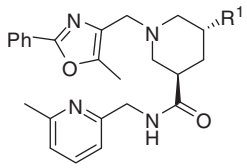

Compound	R^1	IC_{50} (nM)	*c* log *D*
6	H	240	2.9
11	Methyl	40	3.7
12	Ethyl	6	4.2
13	*n*-Propyl	6	4.5
14	*n*-Butyl	15	5.0
15	Phenyl	0.9	4.5
16	CH_2OMe	3.2	2.9
17	OH	2700	3.0
18	OAc	7	3.8
19	OCONHEt	120	3.7

Addition of small alkyl groups at the C-5 position led to an increase in potency with ethyl analog **12** providing the optimal balance of potency and lipophilicity. More potent derivatives could be made (**15**) at the expense of lipophilicity and molecular weight. Compound **12** showed similar potency and selectivity to **2**, however, unlike **2** it did not produce reactive metabolites. The primary liability of **12** was its poor microsomal stability, contributing to high in vivo clearance and low oral bioavailability.[12] This result was not unexpected given the compound's high log *D* of 4.2.[13] Metabolite identification studies showed that multiple sites underwent microsomal oxidation. Given the modular nature of the lead, our goal was to identify more polar replacements for each of its three segments as a means to reduce microsomal metabolism. In order to make more significant changes to log *D*, a matrix set of 22 compounds was designed by combining two or three of the new building blocks. Data for selected compounds is shown in Table 3.[14]

Table 3
PDE8B activity of selected matrix compounds

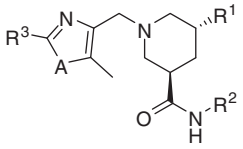

Compound	R^1	R^2	R^3	A	IC_{50} (nM)	*c* log *D*	HLM Cl_{int}
20	Ethyl	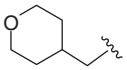	Ph	O	7.3	3.6	320
21	CH_2OMe	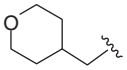	Ph	O	2.0	2.6	240
22	Ethyl	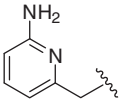	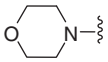	O	17	1.9	110
23	CH_2OMe	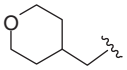	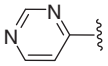	NH	13	0.64	63
24	CH_2OMe	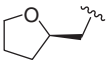	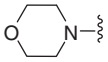	O	65	0.91	41
25	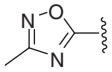	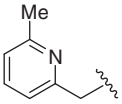	Ph	O	3.9	3.0	105
26	Ethyl	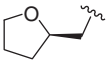	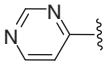	NH	26	1.6	190
27[a]	H	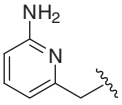	Ph	O	58	2.5	49
28[a]	H	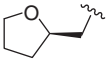	Ph	O	166	2.6	84
29	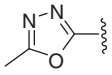	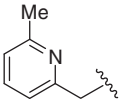	Ph	O	66	2.6	290
30	Ph	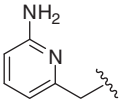	Ph	O	0.12	3.6	>300

[a] Analogs **27** and **28** were tested as single 3*R* enantiomers.

In addition to maintaining potency, other positive attributes of our leads **6** and **12**, such as permeability, aqueous solubility and selectivity over other phosphodiesterases (>1000-fold, except equipotent against PDE8A) were also preserved. Again, the *cis* isomers were inactive. However, microsomal stability was our greatest concern. Figure 5 shows the correlation of *c* log *D* and HLM intrinsic clearance for the set of compounds.

Despite an obvious relationship between *c* log *D* and microsomal clearance (Cl_{int}), reduction of *c* log *D* by four orders of magnitude did not afford potent compounds with low clearance (considered to be <10 μL/min/mg in this assay). Oddly, it was found that the *cis* diastereomers (red markers) were significantly more stable across a broad range of *c* log *D*. The unsubstituted nipecotic amide analogs (R^1 = H, blue markers) displayed clearance values between the *cis* and *trans* isomers. Taken together, these data suggest a conformational component to the metabolism. A similar trend was also observed with RLM (data not shown).

One compound (**24**) from the series was separated into its four component isomers in order to rule out differences between the enantiomers of the core piperidine (Table 4). This compound was chosen based on its properties and the fact that it had the lowest Cl_{int}. Only one of the two *trans* isomers possessed PDE8B inhibitory activity. There was no difference in microsomal clearance between either of the pairs of *cis* or *trans* diastereomers. Experimental pK_a's and log *D*'s were also determined since these parameters, if divergent, could also help to explain the diastereomer-dependent microsomal clearance data. Small but not significant differences in pK_a and log *D* were observed.

Insights into the binding conformation of these inhibitors necessitated the use of homology models due to the inability to crystallize the poorly expressing and difficult to purify PDE8B protein. After numerous docking experiments, a result that accounted for the majority of the known structure activity relationships was identified and is depicted in Figure 6, with **30** as the ligand (Fig. 7). In addition to nicely filling lipophilic pockets, the following interactions are possible. (1) A hydrogen bond from the protonated piperidine NH to Tyr253 (could also be nitrogen lone pair to tyrosine OH). (2) Amide NH hydrogen bond to the backbone carbonyl

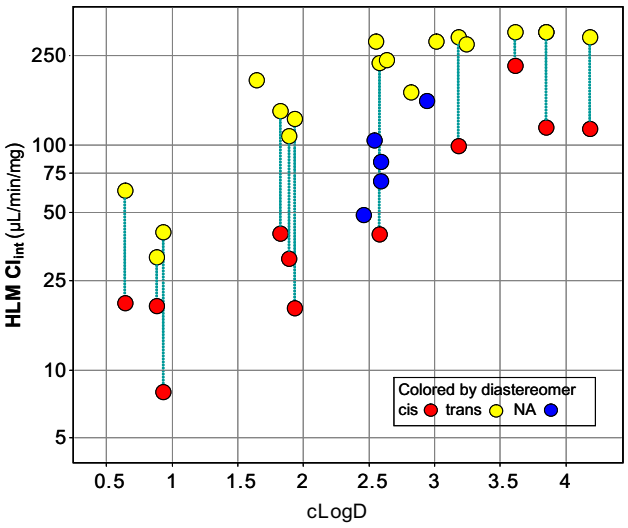

Figure 5. Correlation of microsomal stability versus *c* log *D*. Pairs of diastereomers are connected with dotted lines.

Table 4
Data for individual isomers of **24**

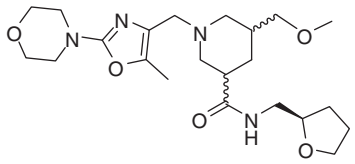

Isomer	PDE8B IC_{50}	HLM Cl_{int}	pK_a	log *D*
trans 1	43 nM	48	7.2	1.0
trans 2	>10 μM	49		1.0
cis 1	>10 μM	<8	7.8	0.8
cis 2	>10 μM	<8		0.8

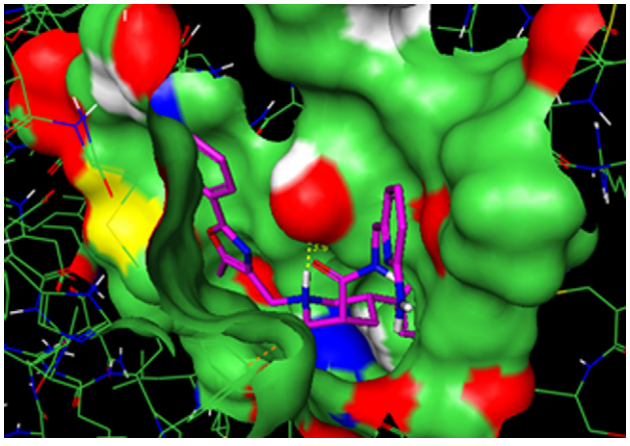

Figure 6. Homology model of **30** binding to PDE8B catalytic domain.

of Pro270. (3) A hydrogen bond from Tyr64 to the oxazole ring oxygen atom, perhaps through a water molecule.

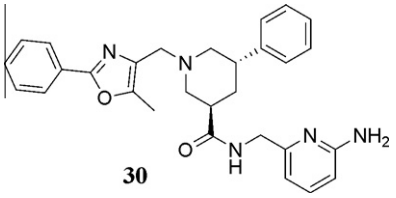

30

Figure 7. Structure of **30** used as the ligand in homology model docking experiments.

This conformation, in which the amide group was in an axial configuration, would be readily accessible in compound **2** given the lack of any A1-3 strain. It would also explain the preference for the *trans* isomer in the nipecotic analogs, since the *cis* isomers would force both substituents in a di-axial arrangement. The absolute configuration of the amide was also the same as the single enantiomer nipecotic amide analogs **27** and **28** further supporting this binding model.

In summary, the first highly potent and selective PDE8 inhibitors have been identified. A scaffold-hopping exercise was successfully utilized to circumvent a reactive metabolite issue. Efforts to reduce microsomal turnover through lowering lipophilicity led to an interesting observation that the *cis* diastereomers were significantly more stable in human microsomes than the *trans*. Although the microsomal clearance of the series was responsive to reductions in lipophilicity, it could not be moved into a range deemed sufficiently low for clinical study. The disclosure and optimization of additional PDE8B scaffolds will be the subject of future publications.

Supplementary data

Supplementary data associated with this article can be found, in the online version, at doi:10.1016/j.bmcl.2011.03.022.

References and notes

1. Hayashi, M.; Matsushima, K.; Ohashi, H.; Tsunoda, H.; Murase, S.; Kawarada, Y.; Tanaka, T. *Biochem. Biophys. Res. Commun.* **1998**, *250*, 751.
2. Soderling, S. H.; Bayuga, S. J.; Beavo, J. A. *Proc. Natl. Acad. Sci. U.S.A.* **1998**, *95*, 8991.
3. Soderling, S. H.; Bayuga, S. J.; Beavo, J. A. *J. Biol. Chem.* **1998**, *273*, 15553.
4. Dov, A.; Abramovitch, E.; Warwar, N.; Nesher, R. *Endocrinology* **2008**, *149*, 741.
5. Horvath, A.; Giatzakis, C.; Tsang, K.; Greene, E.; Osorio, P.; Boikos, S.; Libè, R.; Patronas, Y.; Robinson-White, A.; Remmers, E.; Bertherat, J.; Nesterova, M.; Stratakis, C. A. *Eur. J. Genet.* **2008**, *16*, 1245.
6. Pyne, N. J.; Furman, B. L. *Diabetologia* **2003**, *46*, 1179.
7. Pratley, R. E.; Gilbert, M. *Rev. Diabet. Stud.* **2008**, *5*, 73.
8. Such isoform selectivity has been a major issue in past PDE research, due to a highly conserved catalytic domain among PDE family; see: Ke, H.; Wang, H. *Curr. Top. Med. Chem.* **2007**, *7*, 391.
9. Selectivity was >1000-fold for all other PDE isoforms except PDE8A (IC_{50} = 1.8 nM).
10. The isoquinoloinium species **3** was identified upon incubation with human liver microsomes, and was shown to alkylate glutathione in this assay. See Mutlib, A. E.; Shockcor, J. P. (2003) In *Drug Metabolizing Enzymes-Cytochrome P450 and Other Enzymes in Drug Discovery and Development* Lee, J.S.; Obach, R. S.; Fisher, M.B., Eds.; Fontis Media, S.A., Lausanne, Switzerland, p 33.
11. Unless otherwise noted and where applicable, compounds were tested as diastereomerically pure racemic mixtures. Analogs containing an enantiomerically pure amide substituent (e.g., **24**) were mixtures of diastereomers.
12. Rat PK for compound **12**: Cl = 98 ml/min/kg; V_{dss} = 1.4 L/kg; *F* = 7%; rat PK for compound **24**: Cl = 146 ml/min/kg; V_{dss} = 2.1 L/kg.
13. van de Waterbeemd, H.; Smith, D. A.; Jones, B. C. *J. Comput. Aided Mol. Des.* **2001**, *15*, 273.
14. Data for the complete set of analogs can be found in the Supplementary data.